NIH Public Access
Author Manuscript
J Comp Neurol. Author manuscript; available in PMC 2013 October 03.

Published in final edited form as:
J Comp Neurol. 2008 June 20; 508(6): 927–939. doi:10.1002/cne.21703.

Subcellular Distribution of the Rho-GEF Lfc in Primate Prefrontal Cortex: Effect of Neuronal Activation

E. Chris Muly[1,2,*], **Angus C. Nairn**[3,4], **Paul Greengard**[3], and **Donald G. Rainnie**[1]

[1]Department of Psychiatry and Behavioral Sciences, The Rockefeller University, New York, NY 10021

[2]Division of Neuroscience, Yerkes National Primate Research Center, The Rockefeller University, New York, NY 10021

[3]Laboratory of Molecular and Cellular Neuroscience, The Rockefeller University, New York, NY 10021

[4]Dept. Psychiatry, Yale University School of Medicine, New Haven, CT 06508

Abstract

The strength of synaptic connections in the brain varies with activity and this plasticity depends on remodeling of the actin cytoskeleton in dendritic spines. Critical to this are the Rho family GTPases, whose activity is controlled by various modulatory proteins including the Rho GEF, Lfc. In cultured neurons and non-neuronal cells, Lfc has been shown to both bind to microtubules and to regulate the actin cytoskeleton. Significantly, Lfc was found to be concentrated in the dendritic shafts of cultured hippocampal neurons under control conditions but then translocated into spines when neural activity was stimulated. In this study, we used immunohistochemistry and electron microscopy to examine activity dependent changes in the distribution of Lfc in the neuropil of monkey prefrontal cortex. We found that while Lfc was concentrated in dendrites, it also had a complex distribution in the neuropil, including being present in spines, axons, terminals and glial processes. Moreover, Lfc distribution varied in different layers of cortex. Using an in vitro slice preparation of monkey prefrontal cortex, we demonstrated an activity dependent translocation of Lfc from dendritic shafts to spines. The results of this study support a role for Lfc in activity-dependent spine plasticity and demonstrate the feasibility of studying activity dependent changes in protein localization in tissue slices.

Indexing terms

dendritic spines; neuronal plasticity; actin; ultrastructure; immunoelectron microscopy; in vitro; electrophysiology

---

The regulation of the actin cytoskeleton of dendritic spines is important, not only for spine morphogenesis during development, but also for the creation of new spines in the adult brain and for synaptic plasticity in existing spines. For example, long-term potentiation and long-term depression are associated with changes in spine size and number, and both forms of synaptic plasticity modulate actin polymerization within spines (Star et al., 2002; Fukazawa et al., 2003; Popov et al., 2004; Zhou et al., 2004; Tada and Sheng, 2006). Although the regulation of actin dynamics is complex, the Rho family of small GTPases are thought to play a critical role. The Rho GTPases, which include RhoA, Rac and Cdc42, have distinct

[*]Corresponding Author: E. Chris Muly, Yerkes Primate Research Center, 954 Gatewood Road NE, Atlanta, GA 30329, (404) 727-9603, Fax: (404) 727-3278, ecmuly@rmy.emory.edu.

NIH-PA Author Manuscript
NIH-PA Author Manuscript
NIH-PA Author Manuscript

NIH-PA Author Manuscript

NIH-PA Author Manuscript

NIH-PA Author Manuscript

effects on actin polymerization and neuronal morphology (Nakayama et al., 2000; Tashiro et al., 2000). The actions of these proteins are, in turn, regulated by guanine nucleotide exchange factors (GEFs) and GTPase activating proteins (GAPs), and there is growing appreciation for the role of these proteins in mediating synaptic plasticity (Kins et al., 2000; Penzes et al., 2003; Meng et al., 2003; Van de Ven et al., 2005; Kennedy et al., 2005; Carlisle and Kennedy, 2005; Calabrese et al., 2006).

The protein Lfc (Lbc [lymphoid blast crisis]'s first cousin) was originally identified from a mouse cDNA library in an oncogenic transformation assay (Whitehead et al., 1995), and was observed to contain a putative GEF domain and a pleckstrin homology domain. An Lfc homologue was later identified in a human cDNA library and named GEF-H1 (Ren et al., 1998), which differed from Lfc by the addition of a C-terminal coiled-coil domain. Significantly, this protein interacts with the Rho GTPases, Rac and RhoA, but can serve as a GEF only for RhoA (Glaven et al., 1996). Subsequently, Lfc has been shown to modulate RhoA regulation of the cytoskeleton in various contexts, including meiosis/mitosis (Aijaz et al., 2005; Bakal et al., 2005; Keady et al., 2007) and apoptosis (Chang and Lee, 2006). In non-neuronal cells, Lfc has been shown to bind to microtubules where it is thought to be relatively inactive. Disruption of microtubules leads to activation of Rho by Lfc and to alteration of the actin cytoskeleton (Westwick et al., 1998; Krendel et al., 2002).

In cultured neurons, Lfc is found in dendritic shafts where it associates with microtubules. Intriguingly, when neuronal activity is stimulated, Lfc translocates into dendritic spines where it is believed to play a role in spine plasticity by increasing spine density and decreasing spine length and area (Ryan et al., 2005). Moreover, the activity-dependent modulation of spine morphology is itself dependent on an interaction between Lfc and the actin binding proteins spinophilin and neurabin (Ryan et al., 2005). Alterations in prefrontal spine morphology have been implicated in chronic stress (Radley et al., 2006), psychostimulant use (Robinson and Kolb, 1999; Robinson et al., 2001) and cognitive impairment in ageing (Hao et al., 2006; Hao et al., 2007).

We have previously examined the localization of spinophilin and neurabin in the primate prefrontal cortex (PFC) (Muly et al., 2004a; Muly et al., 2004b) and found that they are concentrated in dendritic spines. In this study, we first sought to determine the basal distribution of Lfc in the primate PFC, and then to determine if this localization could be altered in an activity-dependent manner. Here, we used immunoelectron microscopy and *in vitro* slice physiology to determine the pattern of localization of Lfc in monkey PFC, and then to study the effects of altering synaptic activity on this localization.

Materials and Methods

Animals and Preparation of Tissue

These experiments were performed on prefrontal cortex (Walker's area 9) obtained from 10 macaque monkeys. For experiments in perfusion fixed animals, seven young adult monkeys (aged 3.5 to 9 years) were deeply anesthetized with an overdose of pentobarbital (100 mg/kg), the animals were transcardially perfused, first with Tyrode's solution (137 mM NaCl, 2.7 mM KCl, 1 mM $CaCl_2$, 0.5 mM $MgCl_2$, 12 mM $NaHCO_3$, 0.5 mM NaH_2PO_4, 5 mM glucose) in which 95% O_2/5% CO_2 was bubbled continuously and then with fixative solution consisting of 4% paraformaldehyde/0.1-0.2% glutaraldehyde/0-0.2% picric acid in phosphate buffer (0.1 M, pH 7.4; PB). The brain was then blocked and post fixed in 4% paraformaldehyde for 4 hours. Coronal, 50 μm thick vibratome sections of the prefrontal cortex were cut and then stored frozen at −80°C in 15% sucrose until immunohistochemical labeling was performed.

NIH-PA Author Manuscript

NIH-PA Author Manuscript

NIH-PA Author Manuscript

For *in vitro* slice experiments, three young macaques, aged 1 year 4 months to 1 year 10 months, were used. Younger animals were used to maximize the viability of the tissue slices. The animals used for the *in vitro* slice experiments had all been selected by the Yerkes veterinary staff for sacrifice for clinical reasons (typically chronic diarrhea and failure to thrive). Animals were administered intravenous pentobarbital to produce a deep level of anesthesia, and the level of anesthesia was monitored throughout by a veterinarian. Immediately prior to euthanasia, a large craniotomy was made and the dura incised, additional pentobarbital was then administered to overdose the animal (final dose is 100 mg/kg or higher). The brain was immediately and rapidly removed and processed as described below.

The care of the animals and all anesthesia and euthanasia procedures in this study were performed according to the National Institutes of Health Guide for the Care and Use of Laboratory Animals, and were approved by the Institutional Animal Care and Use Committee of Emory University.

Immunoperoxidase Labeling

Single label immunoperoxidase staining was performed using an affinity purified guinea pig antiserum prepared against a recombinant protein comprised of glutathione *S*-transferase conjugated to amino acids 701-958 of Lfc (Ryan et al., 2005).

Pre-embedding immunoperoxidase labeling was performed as described previously (Muly et al., 2003). Briefly, sections were thawed, incubated in blocking serum (3% normal goat serum, 1% bovine serum albumin, 0.1% glycine, 0.1% lysine in 0.01 M phosphate buffered saline, pH 7.4) for one hour and then placed in the primary antiserum diluted 1:500 in blocking serum. After 36 hours at 4°C, the sections were removed from the primary antiserum, rinsed and placed in a 1:200 dilution of biotinylated goat anti-guinea pig IgG (Vector, Burlingame, CA) for one hour at room temperature. The sections were then rinsed, placed in avidin-biotinylated peroxidase complex for one hour (Vector) and processed to reveal peroxidase using 3,3′-diaminobenzidine (DAB) as the chromogen. Sections that were to be processed for electron microscopy were then osmicated, dehydrated and embedded in Durcupan resin (Electron Microscopy Sciences, Fort Washington, PA). Selected regions were then mounted on blocks and ultrathin sections were collected onto pioloform-coated slot grids and counterstained with uranyl acetate and lead citrate. Control sections, processed as above except for the omission of the primary immunoreagent, did not contain DAB label on electron microscopic examination.

Images of immunolabeled material were captured on a Leica DMRBE microscope using a Spot RT color digital camera (Diagnostic Instruments, Inc., Sterling Heights, MI). Images in TIFF format were imported into an image processing program (Canvas 8, Deneba Software, Miami). The contrast and brightness of the images was adjusted and labels were added. For laminar boundaries, the coverslips were removed and the slides counterstained with thionin.

Analysis of Material

Blocks of tissue were prepared from cortical layers I, III and V of area 9. Ultrathin sections from these blocks were examined using a Zeiss EM10C electron microscope. Regions of the grids containing neuropil were selected based on the presence of label and adequate ultrastructural preservation. In particular, we examined regions that were approximately one micron or more deep to the tissue resin interface. At this depth, ultrastructure was good and label was present but not so strong as to completely obscure ultrastructural features, as was sometimes the case at the surface of the section. We randomly selected fields of immunoreactive elements in the neuropil, and electron micrographs were taken at a

NIH-PA Author Manuscript

NIH-PA Author Manuscript

NIH-PA Author Manuscript

magnification of 31,500. Data were collected from one to three blocks from each layer in three animals. A total of 591 micrographs representing 3,608 μm^2 were taken. On each micrograph, DAB-labeled profiles were identified and classified as spines, dendrites, terminals, axons, glia or unknown based on ultrastructural criteria (Peters et al., 1991). Profiles were identified as spines based on size (0.3 - 1.5 μm in diameter), presence of spine apparatus, absence of mitochondria or microtubules and in some cases the presence of asymmetric synaptic contacts. Dendrites were identified by their larger size (0.5 μm or greater in diameter), presence of microtubules, mitochondria and, in some cases, synaptic contacts. Axon terminals were characterized by the presence of numerous vesicles, mitochondria and occasionally a presynaptic specialization. Pre-terminal, unmyelinated axons were identified by their small size (0.1 – 0.3 μm in diameter), regular round shape and occasional presence of synaptic vesicles or neurofilaments. Glial profiles were identified based on their unusual shape, which appears to fill in the space between other, nearby profiles, and a relatively clear cytoplasm which occasionally contained numerous filaments. Profiles that could not be clearly characterized based on these criteria were considered unknown profiles. The number of immunoreactive profiles was tabulated, and the distributions in different layers compared with a Chi-square analysis.

In Vitro Slice Experiments

The methods for obtaining *in vitro* brain slices were similar to those described previously in rodents (Rainnie, 1999; Rainnie et al., 2006). Briefly, blocks of unfixed prefrontal cortical tissue were placed into oxygenated ice cold “cutting” aCSF (130 mM NaCl, 30 mM $NaHCO_3$, 3.5 mM KCl, 1.1 mM KH_2PO_4, 6 mM $MgCl_2$, 1 mM $CaCl_2$, 10 mM glucose) supplemented with 5 mM kynurenic acid to minimize glutamate-induced neurotoxicity. Tissue blocks were then glued to the stage of an OTS 4000 vibratome (Electron Microscopy Instruments) and 350 μm coronal slices of monkey dorsolateral PFC were sectioned and placed in oxygenated “cutting” aCSF at 32°C for 1 hour to recover from the sectioning procedure prior to experimentation.

In each experiment, available slices were divided into two groups, the “Quiet” and “Stimulated” groups. Following the one hour recovery period, slices in the Stimulated group were transferred into “control” aCSF for 30 minutes. The control aCSF did not contain kynurinate and differed from the cutting aCSF only in having 1.3 mM $MgCl_2$ and 2.5 mM $CaCl_2$. The Stimulated slices were then transferred to a control aCSF containing 10 μM NMDA and 30 μM picrotoxin for 15 minutes. After this stimulation period, the slices were transferred back into control aCSF for 30 minutes and then placed in the perfusion fixative solution for four hours. The Quiet group of slices were kept in the cutting aCSF containing 5mM kynurinate for the same duration as the Stimulated group and then fixed. All slices were continuously oxygenated with 95% oxygen/5% carbon dioxide until fixation. The fixed slices were then resectioned to 50-70 μm on an OTS 4000 vibratome and then frozen in cryoprotectant for subsequent processing for Lfc immunoreactivity, as described above.

Electrophysiological Recordings

Four sample slices were placed in a Warner Series 20 recording chamber (Warner Instruments, Hamden, CT) mounted on the fixed stage of a Leica DM-LFS microscope (Leica Microsystems). Slices were fully submerged and continuously perfused at a rate of 1-2 ml per min with heated (32°C) and oxygenated control ACSF. Neurons were visualized using infrared (IR) illumination and a 40× water immersion objective (Leica Microsystems). Images were captured using an IR sensitive charge-coupled device (CCD) digital camera (Orca ER, Hamamatsu, Tokyo Japan) coupled to a Meteor-II video frame grabber (Matrox Electronic Systems Ltd, Dorval, Canada), and displayed on a computer monitor using Simple PCI 6.11 software (Compix Inc., Cranberry Township, PA).

NIH-PA Author Manuscript

NIH-PA Author Manuscript

NIH-PA Author Manuscript

For whole-cell patch-clamp recording, thin walled borosilicate glass patch electrodes (WPI, Sarasota, Fl.) were pulled on a Flaming/Brown micropipette puller (Model P-97, Sutter Instruments). Patch electrodes had resistances ranging from 4-8 MΩ, when filled with a standard patch solution that contained (in mM): K-Gluconate (138), KCl (2), $MgCl_2$ (3), phosphocreatine (5), K-ATP (2), NaGTP (0.2), HEPES (10). The patch recording solution was adjusted to a pH of 7.3 with KOH and had a final osmolarity of 280 mOsm. Whole-cell patch clamp recordings were obtained as previously described (Rainnie et al. 2004), using an Axopatch-1D amplifier (Molecular Devices, Sunnyvale, CA), a Digidata 1320A A-D interface, and pClamp 9.2 software (Molecular Devices). In cell-attached mode, patch electrode seal resistance was considered acceptable if it was >1.5 GΩ. Whole-cell patch-clamp configuration was established in current-clamp mode and neurons were excluded from analysis if they showed a resting membrane potential (Vm) more positive than –55 mV, and/or had an action potential that did not overshoot +5 mV. Data from current-clamp recordings were sampled at 10 kHz and filtered at 5 kHz.

Drugs were applied by gravity perfusion at the required concentration in the circulating ACSF. Drugs used included: picrotoxin 30 μM, and N-methyl-D-aspartic acid (NMDA) 10 μM (purchased from Sigma-Aldrich, Saint Louis, MO).

Immunohistochemistry and Analysis of *In Vitro* Slice Material

Blocks of tissue were prepared from layer III of area 9. Ultrathin sections from these blocks were examined as described above. Immunoreactive elements were randomly imaged at a magnification of 31,500. For each slice 50-100 images were analyzed. Profiles were identified as spines, dendrites, terminals or other based on the criteria described above. For each slice, the ratio of labeled spines to labeled dendritic shafts observed was determined (100*number of spines/number of dendrites) such that e.g. 50% indicates half as many labeled spines were observed compared to labeled dendritic shafts. A total of 22 *in vitro* slices were used for these experiments, 11 Quiet and 11 Stimulated. In one Quiet slice, no immunoreactivity was recovered and this slice was dropped from analysis. Given the large number of technical variables that could impact this experiment, a preliminary analysis to detect outliers was performed using the Grubbs' test. For each group, a mean was calculated and then a Z value was calculated for each slice according to the formula Z= (mean – value)/ standard deviation. Slices with a Z value above the critical Z value were omitted from further analysis. For an N of 11 (Stimulated group) the critical Z value was 2.34 and for an N of 10 (Quiet group) the critical Z value was 2.29. One slice in each group was identified as an outlier, giving final group numbers of 9 for the Quiet group and 10 for the Stimulated group. The means of these groups were then compared using a non-paired T test.

Results

We first tested the specificity of our affinity purified antiserum to Lfc by immunoblotting brain extract from wild-type and Lfc knockout mice (Ryan et al., 2005 and unpublished data). The antiserum recognized one protein band in wild-type brain, with an estimated molecular weight of 107 kDa (Fig. 1), and this band was not observed in blots from the Lfc knockout mice suggesting that this antisera labels only Lfc in the mouse brain. Similarly, the Lfc antisera recognized a single protein with an estimated molecular weight of 114 kDa in blots of macaque prefrontal cortex (Fig. 1). These results demonstrate that the antiserum is selective for Lfc and recognizes both rodent and primate forms of the protein.

We next examined sections of macaque PFC which had been immunolabeled for Lfc (Fig. 2). Label consisted of both somatodendritic cellular labeling as well as neuropil staining. Labeled cells were observed throughout cortex; however, layer IV showed a relative paucity of both cellular and neuropil labeling (Fig. 2B). Lfc-immunoreactive (Lfc-IR) neurons

NIH-PA Author Manuscript

NIH-PA Author Manuscript

NIH-PA Author Manuscript

typically showed pyramidal cell morphology with stout apical dendrites (Fig. 2B and C). In addition to cells with pyramidal morphology, some smaller Lfc-IR cells were noted (Fig. 2B and C, arrows). Within the neuropil, segments of apical dendrites were seen (Fig. 2C), especially in supragranular layers, in addition to smaller caliber fibers and puncta. These results demonstrate that Lfc-IR is widely distributed in prefrontal pyramidal cells and, perhaps, interneurons. The protein appears to be primarily localized to the soma and dendrites of neurons.

We next used immunoperoxidase electron microscopy to determine the subcellular distribution of Lfc-IR in the neuropil. Neuronal soma were frequently labeled, with patches of immunoperoxidase label in the cytoplasm associated with endoplasmic reticulum (Fig. 3). As expected from the light microscopic examination, dendritic shafts were prominently labeled (Fig. 4). Patches of Lfc-IR were observed within dendrites of a wide range of sizes and this immunolabel often appeared to be associated with the plasma membrane or microtubules within the dendrite. In some cases, the Lfc-IR dendrites were observed to receive asymmetric synapses (Fig. 4B and C). Labeled dendrites were occasionally observed to give rise to dendritic spines (Fig. 4F) indicating that these were the dendrites of pyramidal cells. Dendrites were not the only element labeled in the neuropil and Lfc-IR dendritic spines were also observed (Fig. 4F, 5A). Moreover, labeling was not confined to the dendritic arbor, and Lfc-IR axonal labeling was also observed. Axonal labeling was seen in axon terminals, small pre-terminal unmyelinated axons and large, myelinated axons (Figs. 5B, C, D). Lfc-IR glial processes were also observed (Fig. 5E).

Our qualitative impression on examining the material was that most Lfc-IR elements were dendrites but that the protein was widely distributed in the neuropil. In order to confirm this, we quantified the distribution of immunoreactivity for Lfc in a total of 1167 randomly collected immunoreactive neuropil elements from layers I, III and V in each of three monkeys. The distribution of labeled elements did not vary significantly between the animals (χ^2=12.77, p=0.120), confirming the reproducibility of the distribution. The quantitative distribution of Lfc confirmed our qualitative impression that Lfc is predominately found in dendritic shafts. However, there was a significant difference in the distribution of Lfc label across the three layers examined (χ^2=30.501, p=0.0002; Figure 6). Post hoc testing revealed that the percentage of label found in dendritic shafts was significantly lower in layer V than layers I or III, that terminals were less frequently seen in layer III than layer I, and that labeled axons were less frequently seen in layer I than layer V.

The presence of significant levels of spine localization for Lfc in monkey PFC was of particular interest to us. Previous studies have suggested that the localization of Lfc is highly activity dependent (Ryan et al., 2005). Hence, in primary cultures of rodent hippocampal neurons Lfc is largely localized in the shafts of dendrites; however, Lfc translocates into dendritic spines following glutamate receptor activation. Consequently, we hypothesized that the degree of spine localization compared to dendritic localization in the monkey tissue reflected the level of activity in that brain region prior to sacrifice and perfusion. To test this hypothesis, we prepared *in vitro* slices of macaque PFC and compared Lfc localization in slices exposed to two different levels of synaptic activation. Slices were maintained for two and a quarter hours following removal from the animal. Half the slices were maintained in a "Quiet" condition in which synaptic transmission was almost entirely blocked by incubating in aCSF containing the non-selective glutamate antagonist kynurinate for the period prior to fixation. The rest of the slices, the "Stimulated" condition, were transferred to control aCSF to re-establish baseline synaptic transmission and then stimulated for 15 minutes with a cocktail of NMDA (10 μM) and the GABA antagonist picrotoxin (30 μM) and then transferred back to control aCSF and fixed 30 minutes later.

NIH-PA Author Manuscript

NIH-PA Author Manuscript

NIH-PA Author Manuscript

In a parallel set of slices, we recorded from pyramidal neurons in layer 2/3 of the prefrontal cortex to determine the extent of this treatment on neuronal firing activity and synaptic transmission. We first determined the physiological properties of each neuron tested (N=4) by measuring the voltage response of these neurons to a series of transient depolarizing and hyperpolarizing current steps (Fig. 7C, see also Rainnie et al., 1993). As shown in Table 1, in control aCSF layer 2/3 neurons had properties similar to those previously reported for pyramidal neurons in this region (Henze et al., 2000; Luebke et al., 2004), and elsewhere in the primate brain (Altemus et al., 2005). In control aCSF, baseline synaptic activity consisted of low amplitude (0.6 ± 0.3 mV) excitatory postsynaptic potentials (EPSPs) occurring at ~ 8 Hz (N=238, Fig. 7A). Addition of the NMDA-picrotoxin cocktail (see methods) resulted in a significant increase in the frequency of spontaneous EPSPs (~ 23 Hz) after 2 minutes, and an increase in both frequency and amplitude after 5 minutes, which eventually developed into spontaneous burst firing activity in all neurons tested (n=4; Fig. 7B). The burst firing activity and enhanced EPSP signaling was fully reversible on washout of the NMDA- picrotoxin cocktail (Fig. 7B). These data confirm that our pharmacological treatment induced a significant increase in neuronal activity and synaptic transmission in this treatment group. Moreover, subsequent addition of kynurenic acid almost abolished spontaneous synaptic activity (Fig. 7A, bottom trace).

Subsequent electron microscopic examination of samples from the fixed slices revealed some ultrastructural differences compared with the perfusion material; however, the ultrastructure of these live slices was remarkably well preserved and labeled dendritic spines and shafts were easily identified (Fig. 8). The major ultrastructural difference was widened extracellular spaces in material from the *in vitro* slice and the occasional presence of profiles with dark cytoplasm (Fig. 8C). These latter elements were likely degenerating dendrites or axons, separated from their parent soma by the slicing process.

We then examined Lfc-IR structures randomly imaged from each of the slices. For this analysis, each profile was identified as a spine, a dendritic shaft, terminal or other profile. For our initial analysis, we determined the ratio of observed labeled spines to labeled dendrites for each slice. Consistent with our hypothesis, the ratio of spines to dendrites was significantly higher in slices in which neuronal activity was stimulated, compared to slices in which neuronal activity was suppressed ($t=3.277$, $p=0.0044$; Fig 9A). This suggests that stimulation of synaptic activity leads to a translocation of Lfc from dendritic shafts to spines, as it does in hippocampal cultures. Furthermore, many of the Lfc-IR dendrites observed in Quiet slice material were observed to possess unlabeled spines (Fig. 8B, E). In material from a Stimulated slice, label was observed in the neck of a spine, as if in transit between the shaft and spine (Fig. 8F).

However, a change in spine to dendrite ratio could also result from selective degredation of Lfc in dendrites or a selective increase of expression of Lfc in spines. In order to address this issue we performed a subsequent analysis in which we examined the distribution of Lfc in spines, dendrites and terminals in the two groups of slices. We did not attempt to analyze preterminal axons or glia because of the limitations of the ultrastructural preservation in fixed live slices. We reasoned that if stimulation induces a translocation of Lfc from dendrite to spine, we should see a reduction in the percentage of Lfc found in dendrites and an increase in spines, but that the percentage of the label observed in terminals should not be affected. For additional comparison, we included our perfusion fixed material to examine how Lfc distribution in live slice conditions compared to that from tissue fixed *in situ*. We found that the distribution of Lfc between the three compartments differed significantly between Simulated and Quiet slices and perfusion fixed brain (Fig. 9B; $\chi^2=138.5$, $p<0.0001$). Post-hoc testing confirmed that the percentage of Lfc found in spines and dendrites differed between all three conditions, but that there was no significant difference

NIH-PA Author Manuscript

NIH-PA Author Manuscript

NIH-PA Author Manuscript

in the proportion of Lfc found in axon terminals. The distribution of Lfc in our slices mirrors that seen in perfusion fixed brain, in at least one aspect, and suggests that changing activity levels do not alter the ratio of Lfc localization between the dendritic and axonal compartments. Intriguingly, the ratio of spine to dendrite localization in perfused material was lower than either our Stimulated or Quiet slices. It may be that brain tissue from perfusion fixed material experienced less synaptic activity than our Quiet slice condition, which was obtained from anesthetized animals and went into aCSF with glutamate blockers but in between underwent sectioning which may have stimulated the cells, perhaps through the release of potassium from cut cells. Taken together these results strongly suggest that the localization of Lfc in tissue sections is modulated by neuronal activity, and that this method of analysis provides a means to study activity dependent shifts in protein localization in brain tissue.

Discussion

This study establishes the subcellular distribution of the Rho-GEF, Lfc, in the primate PFC. As observed in hippocampal cultures, our analyses confirm that in brain tissue, Lfc is primarily found in the shafts of dendrites; however, the tissue distribution of Lfc is more complex than could be appreciated in culture preparations. Lfc labeling was observed in dendritic spines as well as in presynaptic compartments. Using a novel combination of *in vitro* slices of primate PFC and immunoelectron microscopy, we found that neuronal activation induces a shift in localization of Lfc from dendritic shafts to dendritic spines.

Lfc, interacts with the both the microtubule (Ren et al., 1998; Glaven et al., 1999; Krendel et al., 2002; Bakal et al., 2005; Callow et al., 2005) and actin cytoskeletons (Glaven et al., 1999; Krendel et al., 2002; Ryan et al., 2005; Callow et al., 2005). Despite the importance of changes in the actin cytoskeleton of dendritic spines for neuronal plasticity, there have been few studies of this protein in neurons (Ryan et al., 2005). This study is the first report of the subcellular distribution of Lfc in brain tissue. As seen in hippocampal cultures (Ryan et al., 2005), Lfc is mainly found in dendritic shafts. However, we also find that Lfc is present in dendritic spines, axon terminals, preterminal axons and some glial processes. There is precedent for the involvement of RhoGEFs in peripheral nerve myelination (Verhoeven et al., 2003; Stendel et al., 2007) and Lfc in CNS glia may regulate myelination or other glial functions. The presence of Lfc in axonal structures suggests that it may have a role in regulating the actin present there (LeBeux and Willemot, 1975; Sankaranarayanan et al., 2003). In particular, the Rho family GTPases and RhoGEFs, including p190RhoGEF and Trio have been shown to play a role in axonal outgrowth, branching, guidance and retraction (Awasaki et al., 2000; Rico et al., 2004; Koh, 2006). Further studies will be required to determine what role, if any, Lfc plays in axonal development or plasticity in the adult nervous system (Gogolla et al., 2007).

Interestingly, the distribution of Lfc is different in different cortical layers. The higher proportion of Lfc found in dendritic shafts in layers I and III compared to layer V may be due to the presence of layer V apical dendrites in superficial layers, in addition to the dendrites of layer II/III pyramidal neurons. Labeled dendrites and spines are over three times more frequently observed than labeled axons or terminals, while in the neuropil, dendrites and spines occupy only 44% more area than axons and terminals (Schuz and Palm, 1989; Braitenburg and Schuz, 1998). This suggests that Lfc is either found more densely throughout the dendritic arbor than the axonal arbor, or that only a subset of axons contain Lfc. The laminar differences observed suggest that Lfc is mainly in the preterminal axon segments of deeper cortical layers, but that it is found in terminals more frequently in layer I. However, the density of synapses does not differ between cortical layers I, III and V in the mouse, suggesting that axon terminals in layer I are relatively enriched with Lfc. Further

NIH-PA Author Manuscript

NIH-PA Author Manuscript

NIH-PA Author Manuscript

work will be required to determine the function of Lfc in axons and the types of axons that contain it.

While Lfc was predominantly localized to dendrites in perfusion fixed material, we were surprised at the degree to which Lfc was also observed in dendritic spines in PFC. Previous studies in hippocampal cultures (Ryan et al., 2005) have suggested that in quiescent neurons, Lfc is found in dendritic shafts; however, it translocates to dendritic spines after activation. While dynamic movements of protein can not be visualized with the methods employed here, we observed that Lfc is mainly found in dendrites in the neuropil of *in vitro* slices in which activity is blocked by glutamate antagonists, but that stimulation of synaptic activity resulted in more Lfc found in dendritic spines than dendritic shafts. These results suggest that activity-dependent shifts in Lfc localization occur not only in culture preparations but also in live slice preparations where local circuitry is relatively preserved.

An important caveat to this work is that spine density may be altered by *in vitro* slice conditions. Kirov and colleagues (1999) found a higher density of synapses in hippocampal slices than in perfusion fixed material. The effect of slice activity on spine number is complex: stimulation does not alter synapse number (Sorra and Harris, 1998), while blockade of activity increases spine density, after 8 hours (Kirov and Harris, 1999). While similar studies have not been done in neocortical slices, we can not rule out the possibility that changes in spine density occur in our PFC slices compared to fixed tissue, and this may affect our comparison between perfusion fixed tissue and slices. Changes in spine number could complicate the interpretation of our data; however, for activity dependent changes in spine density to explain our findings, there would have to be stimulation-induced creation of new spines with Lfc or blockade-induced loss of spines that contain Lfc. The work of Harris and colleagues suggests that if any changes occur in our PFC slices, then our Quiet slices gain spines compared to our Stimulated slices. The effect of the slice environment and activity on PFC slices will require more study, but at this time any changes in spine number do not seem likely to alter our interpretation of our findings.

Thus, the degree to which Lfc is localized in dendritic spines and shafts may represent a marker for the level of neuronal activity in a neuropil region prior to sacrifice. Such a marker would complement the commonly used somatic cFos labeling which is used to identify neurons that have been activated by behavioral or pharmacological challenges (Deutch et al., 1991; Lambert et al., 1996; Schmidt et al., 1996) and might allow for the identification of specific layers of neocortex or hippocampus responsible for altered patterns of synaptic activation. Other activity dependent synaptic markers have been proposed. For example, synaptic stimulation causes newly synthesized mRNA for Arc to be localized selectively to active dendritic regions in hippocampal pyramidal neurons (Steward et al., 1998). Our study does not directly address whether increased activity causes a general shift of Lfc out of dendrites into spines, or if this is specific to activated synapses.

The distribution of Lfc contrasts with that of two interacting proteins, spinophilin and neurabin. Spinophilin and neurabin, which are actin binding scaffolding proteins, are both concentrated in dendritic spines in perfusion fixed material (Muly et al., 2004a; Muly et al., 2004b), while Lfc is concentrated in dendritic shafts. In rat brain, both spinophilin and neurabin co-immunoprecipitate with Lfc, and in cultured N2a cells neurabin and Lfc cluster together at sites that were enriched with actin, but not tubulin (Ryan et al., 2005). This suggests that when associated with each other, Lfc and spinophilin/neurabin are concentrated in dendritic spines, where an actin cytoskeleton predominates. However, spinophilin and neurabin are both found in dendritic shafts as well, though to a lesser degree than in spines (Muly et al., 2004a; Muly et al., 2004b). It remains to be determined whether Lfc first translocates to the spine and then associates with actin binding proteins or if their

NIH-PA Author Manuscript

NIH-PA Author Manuscript

NIH-PA Author Manuscript

interaction can occur in dendrites and is part of the process by which Lfc is translocated to spines.

The finding that Lfc is distributed within prefrontal dendritic arbors in an activity dependent manner supports a role for this protein in modulating the actin cytoskeleton of spines in response to neural activity. The modulation of actin and consequently spine morphology is a critical component of synaptic plasticity, and roughly half of neuronal energy is spent on maintaining a dynamic actin cytoskeleton (Bernstein and Bamburg, 2003). For example, induction of long-term potentiation and long-term depression of synaptic strength are associated with an increase and decrease respectively of both actin polymerization and spine size (Popov et al., 2004; Zhou et al., 2004; Okamoto et al., 2004; Tada and Sheng, 2006; Harms and Dunaevsky, 2006). In addition to Lfc, other proteins have been shown to redistribute between dendritic shafts and spines in an activity-dependent manner. For example β-catenin translocates from the dendritic shaft into spines upon membrane depolarization by an NMDA receptor-dependent mechanism (Murase et al., 2002). This shift of β-catenin results in an increase in spine size, increases the size of PSD-95 clusters in spine heads and appears to increase the amplitude of excitatory synaptic responses (Murase et al., 2002; Takeichi and Abe, 2005; Okuda et al., 2007). Calcium/calmodulin-dependent protein kinase II (CaMKII) also translocates into spines following NMDA receptor stimulation and LTP induction (Otmakhov et al., 2004). Intriguingly, activity induced translocation can occur in both directions. The F-actin binding protein cortactin translocates from spines to dendritic shafts following NMDA receptor stimulation (Hering and Sheng, 2003).

These studies indicate that synaptic activity in general and NMDA receptor activation in particular induce complex changes in the molecular milieu of the dendritic spine that appear likely to correspond to both structural and functional alterations. Lfc's properties as a Rho-GEF and its known interactions with the cytoskeleton and scaffolding proteins suggest it contributes significantly to these alterations. Once translocated to spines, Lfc could stimulate Rho activity and modulate spine morphology (Tada and Sheng, 2006). The interaction between Lfc and the PP1 scaffolding proteins spinophilin and neurabin might alter protein phosphatase-1 (PP1) activity in spines, which in turn could alter glutamate receptor phosphorylation and, hence, synaptic transmission (Mulkey et al., 1994; Thiels et al., 2000; Morishita et al., 2001). The effect of synaptic activation and Lfc translocation will likely depend on the temporal pattern of activation and possibly the degree to which metabotropic glutamate or monoamine receptors are co-activated.

Acknowledgments

The authors gratefully acknowledge the excellent technical assistance of Marcelia Maddox, and Dr. Xiaozhou Ryan for preparation of the antisera and providing a Western blot in knockout mice.

Grant sponsor: National Institutes of Health; Grant numbers: MH01994 (to E.C.M.), MH069852 (to D.G.R.), DA10044 (to P.G. and A.C.N.) and RR00165.

References

Aijaz S, D'Atri F, Citi S, Balda MS, Matter K. Binding of GEF-H1 to the tight junction-associated adaptor cingulin results in inhibition of Rho signaling and G1/S phase transition. Dev Cell. 2005; 8:777–786. [PubMed: 15866167]

Altemus KL, Lavenex P, Ishizuka N, Amaral DG. Morphological characteristics and electrophysiological properties of CA1 pyramidal neurons in macaque monkeys. Neurosci. 2005; 136:741–756.

NIH-PA Author Manuscript

NIH-PA Author Manuscript

NIH-PA Author Manuscript

Awasaki T, Saito M, Sone M, Suzuki E, Sakai R, Ito K, Hama C. The Drosophila trio plays an essential role in patterning of axons by regulating their directional extension. Neuron. 2000; 26:119–131. [PubMed: 10798397]

Bakal CJ, Finan D, LaRose J, Wells CD, Gish G, Kulkarni S, DeSepulveda P, Wilde A, Rottapel R. The Rho GTP exchange factor Lfc promotes spindle assembly in early mitosis. Proc Natl Acad Sci U S A. 2005; 102:9529–9534. [PubMed: 15976019]

Bernstein BW, Bamburg JR. Actin-ATP hydrolysis is a major energy drain for neurons. J Neurosci. 2003; 23:1–6. [PubMed: 12514193]

Braitenburg, V.; Schuz, A. Cortex: Statistics and Geometry of Neuronal Connectivity. Berlin: Springer; 1998.

Calabrese B, Wilson MS, Halpain S. Development and regulation of dendritic spine synapses. Physiology (Bethesda). 2006; 21:38–47. [PubMed: 16443821]

Callow MG, Zozulya S, Gishizky ML, Jallal B, Smeal T. PAK4 mediates morphological changes through the regulation of GEF-H1. J Cell Sci. 2005; 118:1861–1872. [PubMed: 15827085]

Carlisle HJ, Kennedy MB. Spine architecture and synaptic plasticity. Trends Neurosci. 2005; 28:182–187. [PubMed: 15808352]

Chang ZF, Lee HH. RhoA signaling in phorbol ester-induced apoptosis. J Biomed Sci. 2006; 13:173–180. [PubMed: 16496227]

Deutch AY, Lee MC, Gillham MH, Cameron DA, Goldstein M, Iadarola MJ. Stress selectively increases fos protein in dopamine neurons innervating the prefrontal cortex. Cereb Cortex. 1991; 1:273–292. [PubMed: 1668366]

Fukazawa Y, Saitoh Y, Ozawa F, Ohta Y, Mizuno K, Inokuchi K. Hippocampal LTP is accompanied by enhanced F-actin content within the dendritic spine that is essential for late LTP maintenance in vivo. Neuron. 2003; 38:447–460. [PubMed: 12741991]

Glaven JA, Whitehead I, Bagrodia S, Kay R, Cerione RA. The Dbl-related protein, Lfc, localizes to microtubules and mediates the activation of Rac signaling pathways in cells. J Biol Chem. 1999; 274:2279–2285. [PubMed: 9890991]

Glaven JA, Whitehead IP, Nomanbhoy T, Kay R, Cerione RA. Lfc and Lsc oncoproteins represent two new guanine nucleotide exchange factors for the Rho GTP-binding protein. J Biol Chem. 1996; 271:27374–27381. [PubMed: 8910315]

Gogolla N, Galimberti I, Caroni P. Structural plasticity of axon terminals in the adult. Curr Opin Neurobiol. 2007; 17:1–9.

Hao J, Rapp PR, Janssen WG, Lou W, Lasley BL, Hof PR, Morrison JH. Interactive effects of age and estrogen on cognition and pyramidal neurons in monkey prefrontal cortex. Proc Natl Acad Sci U S A. 2007; 104:11465–11470. [PubMed: 17592140]

Hao J, Rapp PR, Leffler AE, Leffler SR, Janssen WG, Lou W, McKay H, Roberts JA, Wearne SL, Hof PR, Morrison JH. Estrogen alters spine number and morphology in prefrontal cortex of aged female rhesus monkeys. J Neurosci. 2006; 26:2571–2578. [PubMed: 16510735]

Harms KJ, Dunaevsky A. Dendritic spine plasticity: Looking beyond development. Brain Res. 2006

Henze DA, Gonzalez-Burgos GR, Urban NN, Lewis DA, Barrionuevo G. Dopamine increases excitability of pyramidal neurons in primate prefrontal cortex. J Neurophysiol. 2000; 84:2799–2809. [PubMed: 11110810]

Hering H, Sheng M. Activity-dependent redistribution and essential role of cortactin in dendritic spine morphogenesis. J Neurosci. 2003; 23:11759–11769. [PubMed: 14684878]

Keady BT, Kuo P, Martinez SE, Yuan L, Hake LE. MAPK interacts with XGef and is required for CPEB activation during meiosis in Xenopus oocytes. J Cell Sci. 2007; 120:1093–1103. [PubMed: 17344432]

Kennedy MB, Beale HC, Carlisle HJ, Washburn LR. Integration of biochemical signalling in spines. Nat Rev Neurosci. 2005; 6:423–434. [PubMed: 15928715]

Kins S, Betz H, Kirsch J. Collybistin, a newly identified brain-specific GEF, induces submembrane clustering of gephyrin. Nat Neurosci. 2000; 3:22–29. [PubMed: 10607391]

Kirov SA, Harris KM. Dendrites are more spiny on mature hippocampal neurons when synapses are inactivated. Nat Neurosci. 1999; 2:878–883. [PubMed: 10491607]

NIH-PA Author Manuscript

NIH-PA Author Manuscript

NIH-PA Author Manuscript

Kirov SA, Sorra KE, Harris KM. Slices have more synapses than perfusion-fixed hippocampus from both young and mature rats. J Neurosci. 1999; 19:2876–2886. [PubMed: 10191305]

Koh CG. Rho GTPases and their regulators in neuronal functions and development. Neurosignals. 2006; 15:228–237. [PubMed: 17409776]

Krendel M, Zenke FT, Bokoch GM. Nucleotide exchange factor GEF-H1 mediates cross-talk between microtubules and the actin cytoskeleton. Nat Cell Biol. 2002; 4:294–301. [PubMed: 11912491]

Lambert PD, Ely TD, Gross RE, Kilts CD. Neurotensin induces Fos and Zif268 expression in limbic nuclei of the rat brain. Neurosci. 1996; 75:1141–1151.

LeBeux YJ, Willemot J. An ultrastructural study of the microfilaments in rat brain by means of heavy meromyosin labeling. I. The perikaryon, the dendrites and the axon. Cell Tissue Res. 1975; 160:1–36. [PubMed: 50139]

Luebke JI, Chang YM, Moore TL, Rosene DL. Normal aging results in decreased synaptic excitation and increased synaptic inhibition of layer 2/3 pyramidal cells in the monkey prefrontal cortex. Neurosci. 2004; 125:277–288.

Meng Y, Zhang Y, Tregoubov V, Falls DL, Jia Z. Regulation of spine morphology and synaptic function by LIMK and the actin cytoskeleton. Rev Neurosci. 2003; 14:233–240. [PubMed: 14513866]

Morishita W, Connor JH, Xia H, Quinlan EM, Shenolikar S, Malenka RC. Regulation of synaptic strength by protein phosphatase 1. Neuron. 2001; 32:1133–1148. [PubMed: 11754843]

Mulkey RM, Endo S, Shenolikar S, Malenka RC. Involvement of a calcineurin/inhibitor-1 phosphatase cascade in hippocampal long-term depression. Nat. 1994; 369:486–488.

Muly EC, Allen P, Mazloom M, Aranbayeva Z, Greenfield AT, Greengard P. Subcellular distribution of neurabin immunolabeling in primate prefrontal cortex: Comparison with spinophilin. CC. 2004a; 14:1398–1407.

Muly EC, Maddox M, Smith Y. Distribution of mGluR1α and mGluR5 immunolabeling in primate prefrontal cortex. J Comp Neurol. 2003; 467:521–535. [PubMed: 14624486]

Muly EC, Smith Y, Allen P, Greengard P. Subcellular distribution of spinophilin immunolabeling in primate prefrontal cortex: localization to and within dendritic spines. J Comp Neurol. 2004b; 469:185–197. [PubMed: 14694533]

Murase S, Mosser E, Schuman EM. Depolarization drives beta-Catenin into neuronal spines promoting changes in synaptic structure and function. Neuron. 2002; 35:91–105. [PubMed: 12123611]

Nakayama AY, Harms MB, Luo L. Small GTPases Rac and Rho in the maintenance of dendritic spines and brances in hippocampal pyramdial neurons. J Neurosci. 2000; 20:5329–5338. [PubMed: 10884317]

Okamoto K, Nagai T, Miyawaki A, Hayashi Y. Rapid and persistent modulation of actin dynamics regulates postsynaptic reorganization underlying bidirectional plasticity. Nat Neurosci. 2004; 7:1104–1112. [PubMed: 15361876]

Okuda T, Yu LM, Cingolani LA, Kemler R, Goda Y. beta-Catenin regulates excitatory postsynaptic strength at hippocampal synapses. Proc Natl Acad Sci U S A. 2007; 104:13479–13484. [PubMed: 17679699]

Otmakhov N, Tao-Cheng JH, Carpenter S, Asrican B, Dosemeci A, Reese TS, Lisman J. Persistent accumulation of calcium/calmodulin-dependent protein kinase II in dendritic spines after induction of NMDA receptor-dependent chemical long-term potentiation. J Neurosci. 2004; 24:9324–9331. [PubMed: 15496668]

Penzes P, Beeser A, Chernoff J, Schiller MR, Eipper BA, Mains RE, Huganir RL. Rapid induction of dendritic spine morphogenesis by trans-synaptic ephrinB-EphB receptor activation of the Rho-GEF kalirin. Neuron. 2003; 37:263–274. [PubMed: 12546821]

Peters, A.; Palay, SL.; Webster, Hd. The Fine Structure of the Nervous System: Neurons and Their Supporting Cells. New York: Oxford University Press; 1991.

Popov VI, Davies HA, Rogachevsky VV, Patrushev IV, Errington ML, Gabbott PL, Bliss TV, Stewart MG. Remodelling of synaptic morphology but unchanged synaptic density during late phase long-term potentiation (LTP): a serial section electron micrograph study in the dentate gyrus in the anaesthetised rat. Neurosci. 2004; 128:251–262.

NIH-PA Author Manuscript

NIH-PA Author Manuscript

NIH-PA Author Manuscript

Radley JJ, Rocher AB, Miller M, Janssen WG, Liston C, Hof PR, McEwen BS, Morrison JH. Repeated stress induces dendritic spine loss in the rat medial prefrontal cortex. Cereb Cortex. 2006; 16:313–320. [PubMed: 15901656]

Rainnie DG. Serotonergic modulation of neurotransmission in the rat basolateral amygdala. J Neurophysiol. 1999; 82:69–85. [PubMed: 10400936]

Rainnie DG, Asprodini EK, Shinnick-Gallagher P. Intracellular recordings from morphologically identified neurons of the basolateral amygdala. J Neurophysiol. 1993; 69:1350–1362. [PubMed: 8492168]

Rainnie DG, Mania I, Mascagni F, McDonald AJ. Physiological and morphological characterization of parvalbumin-containing interneurons of the rat basolateral amygdala. J Comp Neurol. 2006; 498:142–161. [PubMed: 16856165]

Ren Y, Li R, Zheng Y, Busch H. Cloning and characterization of GEF-H1, a microtubule-associated guanine nucleotide exchange factor for Rac and Rho GTPases. J Biol Chem. 1998; 273:34954–34960. [PubMed: 9857026]

Rico B, Beggs HE, Schahin-Reed D, Kimes N, Schmidt A, Reichardt LF. Control of axonal branching and synapse formation by focal adhesion kinase. Nat Neurosci. 2004; 7:1059–1069. [PubMed: 15378065]

Robinson TE, Gorny G, Mitton E, Kolb B. Cocaine self-administration alters the morphology of dendrites and dendritic spines in the nucleus accumbens and neocortex. Syn. 2001; 39:257–266.

Robinson TE, Kolb B. Alterations in the morphology of dendrites and dendritic spines in the nucleus accumbens and prefrontal cortex following repeated treatment with amphetamine or cocaine. Eur J Neurosci. 1999; 11:1598–1604. [PubMed: 10215912]

Ryan XP, Alldritt J, Svenningsson P, Allen PB, Wu GY, Nairn AC, Greengard P. The Rho-specific GEF Lfc interacts with neurabin and spinophilin to regulate dendritic spine morphology. Neuron. 2005; 47:85–100. [PubMed: 15996550]

Sankaranarayanan S, Atluri PP, Ryan TA. Actin has a molecular scaffolding, not propulsive, role in presynaptic function. Nat Neurosci. 2003; 6:127–135. [PubMed: 12536209]

Schmidt U, Beyer C, Oestreicher AB, Reisert I, Schilling K, Pilgrim C. Activation of dopaminergic D1 receptors promotes morphogenesis of developing striatal neurons. Neurosci. 1996; 74:453–460.

Schuz A, Palm G. Density of neurons and synapses in the cerebral cortex of the mouse. J Comp Neurol. 1989; 286:442–455. [PubMed: 2778101]

Sorra KE, Harris KM. Stability in synapse number and size at 2 hr after long-term potentiation in hippocampal area CA1. J Neurosci. 1998; 18:658–671. [PubMed: 9425008]

Star EN, Kwiatkowski DJ, Murthy VN. Rapid turnover of actin in dendritic spines and its regulation by activity. Nat Neurosci. 2002; 5:239–246. [PubMed: 11850630]

Stendel C, Roos A, Deconinck T, Pereira J, Castagner F, Niemann A, Kirschner J, Korinthenberg R, Ketelsen UP, Battaloglu E, Parman Y, Nicholson G, Ouvrier R, Seeger J, De Jonghe P, Weis J, Kruttgen A, Rudnik-Schoneborn S, Bergmann C, Suter U, Zerres K, Timmerman V, Relvas JB, Senderek J. Peripheral nerve demyelination caused by a mutant Rho GTPase guanine nucleotide exchange factor, frabin/FGD4. Am J Hum Genet. 2007; 81:158–164. [PubMed: 17564972]

Steward O, Wallace CS, Lyford GL, Worley PF. Synaptic activation causes the mRNA for the IEG *Arc* to localize selectively near activated postsynaptic sites on dendrites. Neuron. 1998; 21:741–751. [PubMed: 9808461]

Tada T, Sheng M. Molecular mechanisms of dendritic spine morphogenesis. Curr Opin Neurobiol. 2006; 16:95–101. [PubMed: 16361095]

Takeichi M, Abe K. Synaptic contact dynamics controlled by cadherin and catenins. Trends Cell Biol. 2005; 15:216–221. [PubMed: 15817378]

Tashiro A, Minden A, Yuste R. Regulation of dendritic spine morphology by the Rho family of small GTPases: antagonistic roles of Rac and Rho. Cereb Cortex. 2000; 10:927–938. [PubMed: 11007543]

Thiels E, Kanterewicz BI, Knapp LT, Barrionuevo G, Klann E. Protein phosphatase-mediated regulation of protein kinase C during long-term depression in the adult hippocampus *in vivo*. J Neurosci. 2000; 20:7199–7207. [PubMed: 11007876]

NIH-PA Author Manuscript

NIH-PA Author Manuscript

NIH-PA Author Manuscript

Van de Ven TJ, VanDongen HM, VanDongen AM. The nonkinase phorbol ester receptor alpha 1-chimerin binds the NMDA receptor NR2A subunit and regulates dendritic spine density. J Neurosci. 2005; 25:9488–9496. [PubMed: 16221859]

Verhoeven K, De Jonghe P, Van de PT, Nelis E, Zwijsen A, Verpoorten N, De Vriendt E, Jacobs A, Van G V, Francis A, Ceuterick C, Huylebroeck D, Timmerman V. Slowed conduction and thin myelination of peripheral nerves associated with mutant rho Guanine-nucleotide exchange factor 10. Am J Hum Genet. 2003; 73:926–932. [PubMed: 14508709]

Westwick JK, Lee RJ, Lambert QT, Symons M, Pestell RG, Der CJ, Whitehead IP. Transforming potential of Dbl family proteins correlates with transcription from the cyclin D1 promoter but not with activation of Jun NH2-terminal kinase, p38/Mpk2, serum response factor, or c-Jun. J Biol Chem. 1998; 273:16739–16747. [PubMed: 9642229]

Whitehead I, Kirk H, Tognon C, Trigo-Gonzalez G, Kay R. Expression cloning of lfc, a novel oncogene with structural similarities to guanine nucleotide exchange factors and to the regulatory region of protein kinase C. J Biol Chem. 1995; 270:18388–18395. [PubMed: 7629163]

Zhou Q, Homma KJ, Poo MM. Shrinkage of dendritic spines associated with long-term depression of hippocampal synapses. Neuron. 2004; 44:749–757. [PubMed: 15572107]

NIH-PA Author Manuscript

NIH-PA Author Manuscript

NIH-PA Author Manuscript

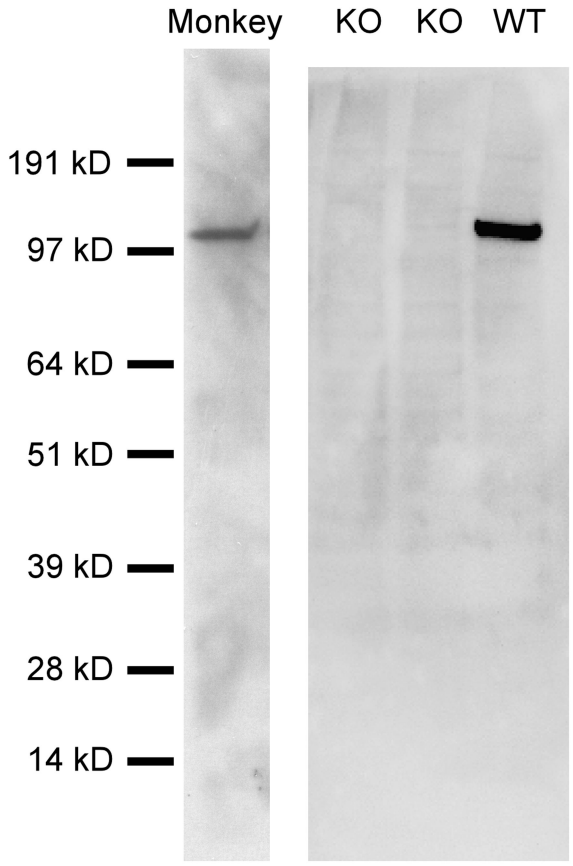

Figure 1.
Western blots demonstrating the specificity of the Lfc antisera. Western blots on brain homogenates from mice in which the Lfc gene had been knocked out (KO) or was not perturbed (WT), as well as homogenates of macaque prefrontal cortex (Monkey) were performed. A single band was recognized in WT mice which ran at an estimated 107 kD and this band was absent in KO mouse brain tissue. In macaque PFC, a single band was recognized by the Lfc antisera with an apparent molecular weight of 114 kD.

NIH-PA Author Manuscript
NIH-PA Author Manuscript
NIH-PA Author Manuscript

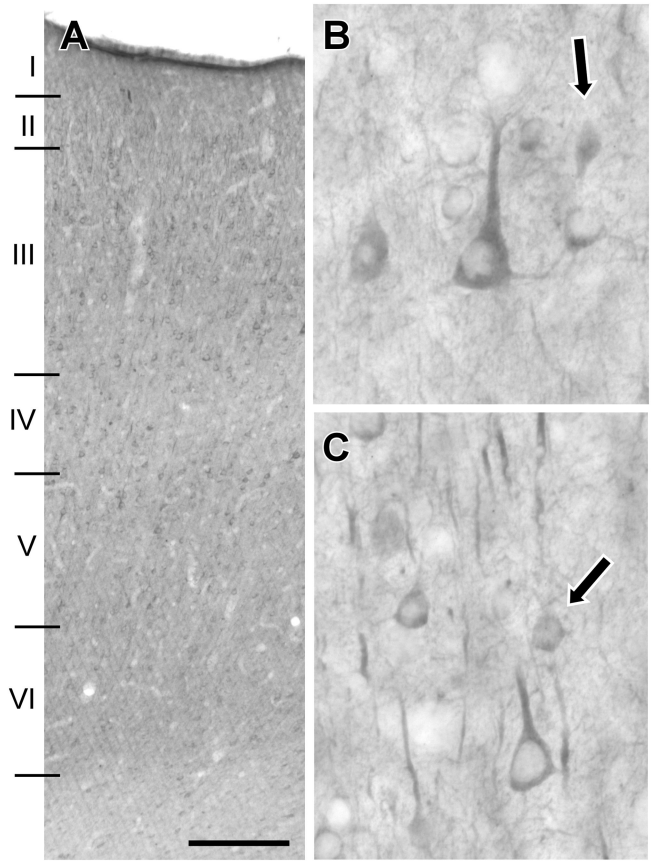

Figure 2.

Lfc labeling of macaque PFC. Lfc-IR labeled cell bodies and dendritic segments are present throughout the depth of PFC and are relatively evenly distributed with the exception of layer IV, in which relatively few labeled cell bodies are observed (A). At higher magnification, Lfc-IR cell bodies are seen to exhibit a pyramidal morphology (B, C), though smaller labeled cells which might be interneurons are also observed (arrows, B, C). Labeling in the neuropil consists of strongly labeled processes that appear to be apical dendritic segments, but a more fine fibrillary and punctate label is also observed (B,C). Scale bar represents 250 μm (A) and 30 μm (B, C).

NIH-PA Author Manuscript

NIH-PA Author Manuscript

NIH-PA Author Manuscript

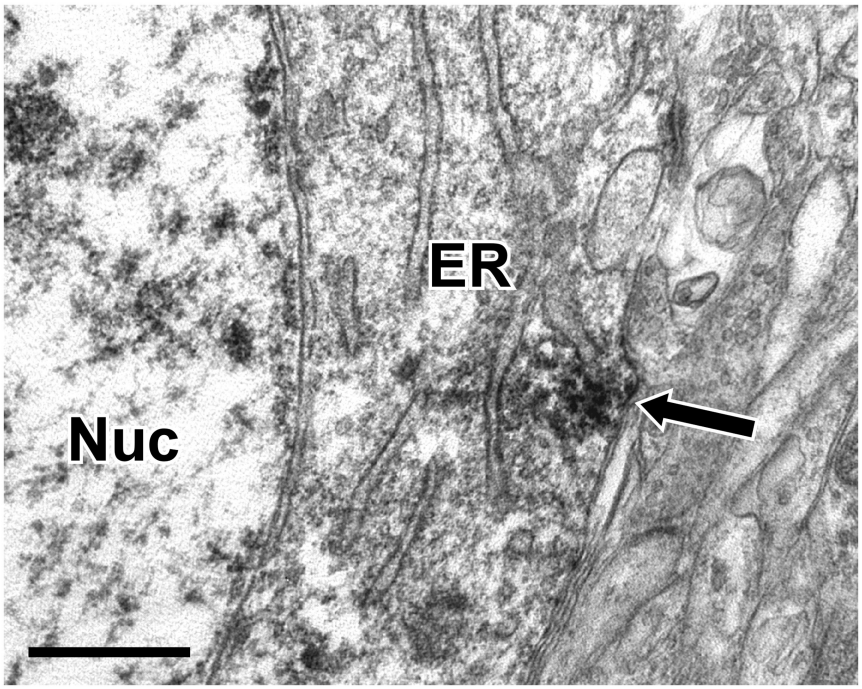

Figure 3.
Electron micrograph illustrating Lfc immunoreactivity in neuronal somata of PFC. Immunoperoxidase reaction product (arrow) was frequently observed in the cytoplasm of neurons and was typically associated with the endoplasmic reticulum. Endoplasmic reticulum (ER), Nucleus (Nuc), Scale bar is 500 nm.

NIH-PA Author Manuscript
NIH-PA Author Manuscript
NIH-PA Author Manuscript

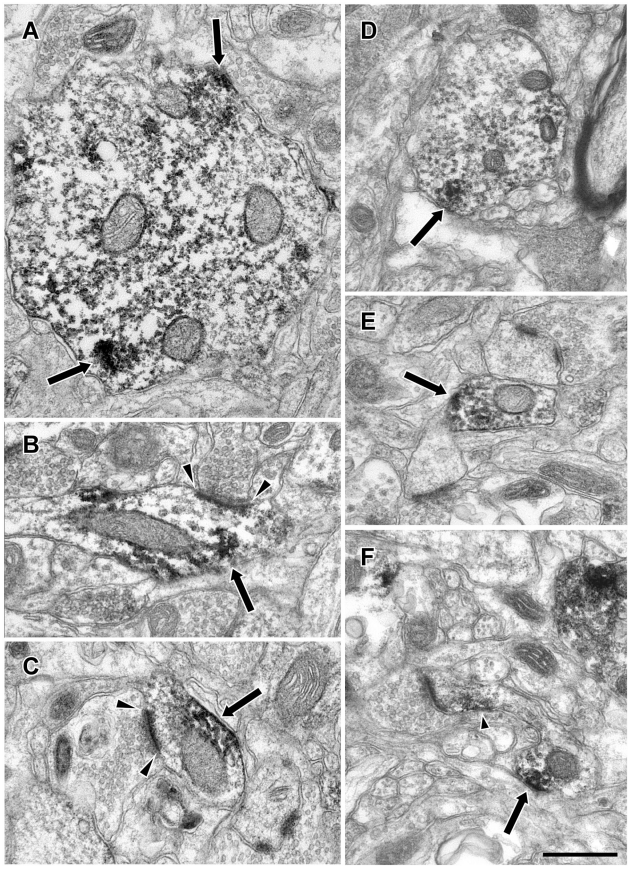

Figure 4.
Electron micrographs illustrating Lfc immunoreactivity in dendrites of the PFC. Lfc-IR (arrows) was observed in dendrites of different sizes including large (A), medium (D) and small caliber dendrites (E). These patches of immunoreactivity were often associated with the plasma membrane or with dendritic microtubules. Some dendritic profiles were observed to receive asymmetric synaptic contacts (arrowheads, B and C). Occasionally, Lfc-IR dendrites were observed to give rise to dendritic spines that were themselves, sometimes labeled (small arrowhead, F). Scale bar is 500 nm.

NIH-PA Author Manuscript

NIH-PA Author Manuscript

NIH-PA Author Manuscript

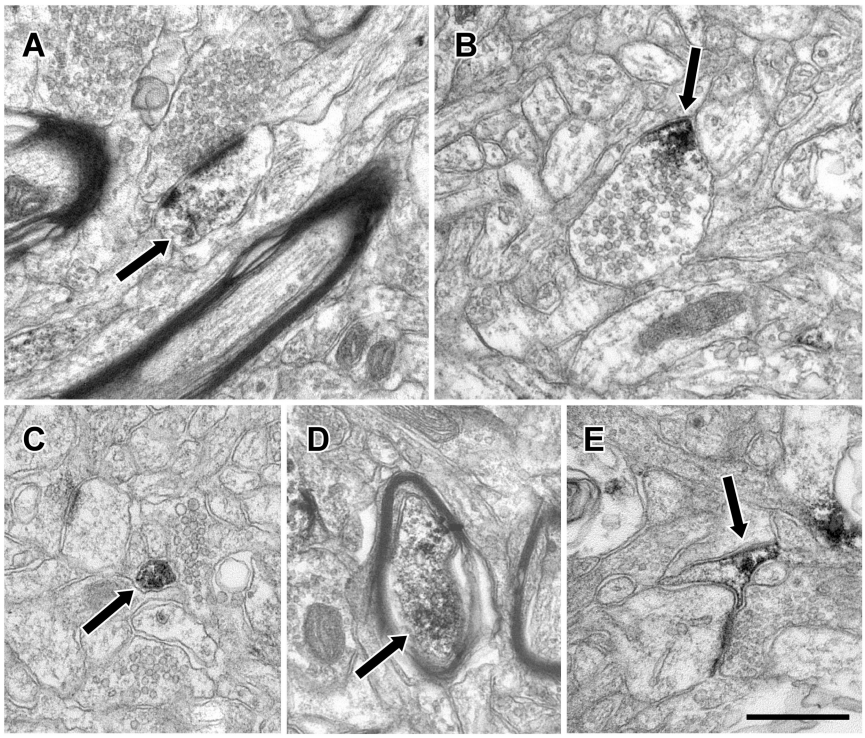

Figure 5.
Electron micrographs illustrating Lfc immunoreactivity in the neuropil of PFC. Lfc-IR (arrows) was observed in diverse elements of the neuropil including dendritic spines (A), axon terminals (B), preterminal axons (C), myelinated axons (D) and glial processes (E). Scale bar is 500 nm.

NIH-PA Author Manuscript

NIH-PA Author Manuscript

NIH-PA Author Manuscript

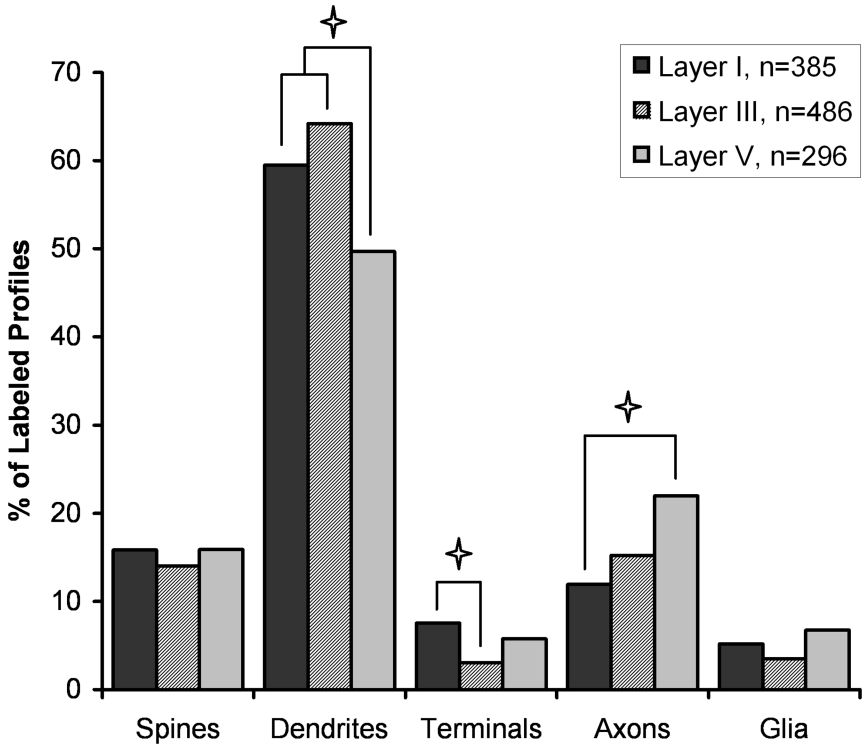

Figure 6.

Histogram showing the relative abundance of Lfc elements in the neuropil of layers I, III and V of monkey PFC. This graph represents a total of 385 labeled elements in layer I, 486 elements in layer III and 296 elements in layer V. The distribution of Lfc labeled profiles differs significantly between the three cortical layers (χ^2=30.501, p=0.0002). Post hoc testing demonstrated significantly less Lfc label found in dendrites of layer V compared to layers I and III, less Lfc in axon terminals in layer III compared to layer I, and more Lfc in preterminal axons in layer V, compared to layer I ($p < 0.05$, denoted by asterisks).

NIH-PA Author Manuscript

NIH-PA Author Manuscript

NIH-PA Author Manuscript

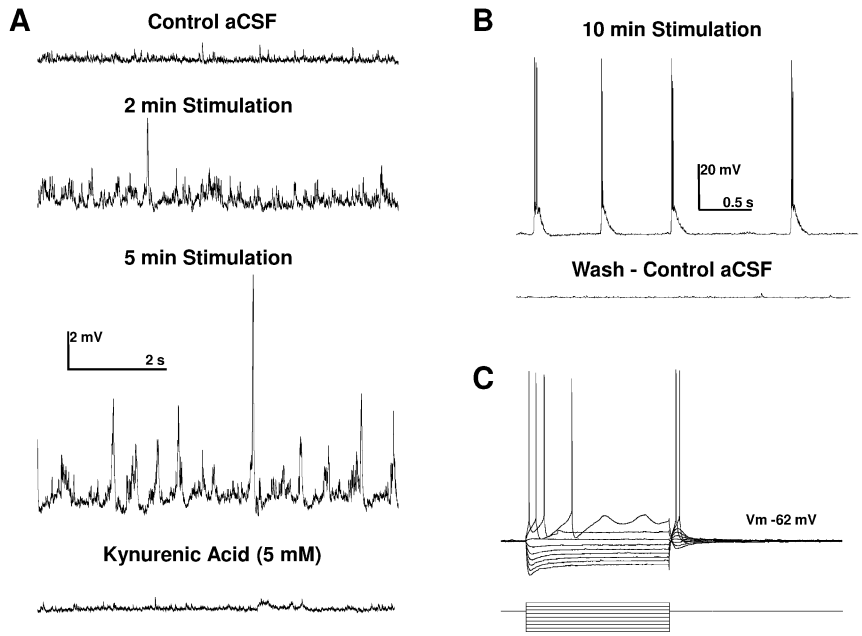

Figure 7.

Pharmacological blockade of $GABA_A$ receptors and concurrent activation of N-methyl-D-aspartate (NMDA) receptors caused a time-dependent increase in spontaneous excitatory postsynaptic potentials (EPSPs) recorded in putative layer 3 projection neurons recorded from the medial prefrontal cortex of the rhesus macaque. A: Application of bicuculline methiodide (30 μM) and NMDA (10 μM) to the superfusion aCSF caused a time dependent increase in the frequency and amplitude of spontaneous EPSPs in mPFC projection neurons. B: After 10 minutes stimulation EPSPs were seen to summate and reach threshold to drive bursts of action potentials in all mPFC projection neurons tested (N=4), an effect that was reversible on washout with control aCFS. C: A typical current clamp recording from a putative layer 3 mPFC projection neuron showing the voltage response (upper trace) to a series of transient (750 ms) current steps (lower trace, range -1 nA to +350 pA).

NIH-PA Author Manuscript
NIH-PA Author Manuscript
NIH-PA Author Manuscript

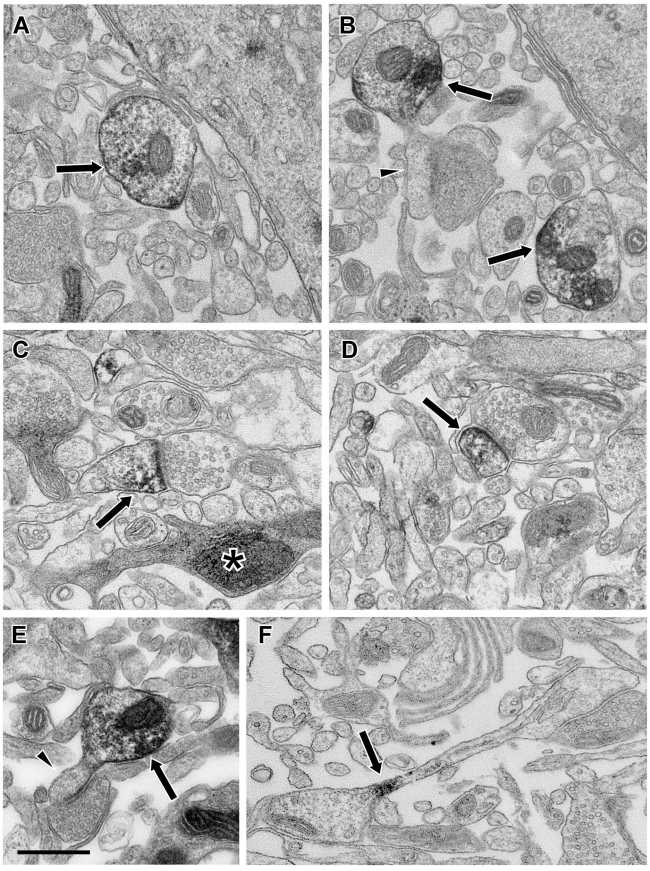

Figure 8.

Electron micrographs illustrating Lfc immunoreactivity from *in vitro* slices of primate PFC. The ultrastructure from the slice material showed some widened extracellular spaces and occasional profiles with dark, condensed cytoplasm (asterisk, C), but was otherwise good and labeled elements could be identified based on morphological criteria. In material from Quiet slices, Lfc-IR (arrows) was observed frequently in dendritic shafts (A, B, E) and some of these dendrites were observed to give rise to unlabeled spines (arrowheads, B, E). In Stimulated slices, Lfc-IR (arrows) was more frequently observed in spines (C, D). Occasionally Lfc-IR could be observed in spine necks (F), as if in transit between the shaft and spine. Scale bar is 500 nm.

NIH-PA Author Manuscript

NIH-PA Author Manuscript

NIH-PA Author Manuscript

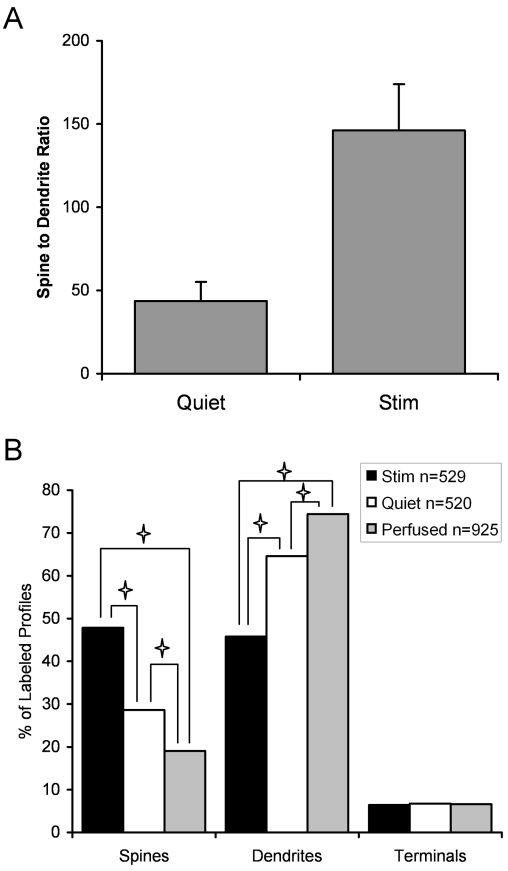

Figure 9.

Histogram showing the effect of activity on the localization of Lfc. A: The ratio of labeled spines to dendrites was determined in *in vitro* slices maintained in a Quiet condition, where synaptic activity was blocked by a glutamate antagonist (n=9) and in slices stimulated by NMDA and picrotoxin (n=10). The ratio of labeled spines to dendrites was significantly higher in Stimulated slices compared to Quiet slices ($t=3.277$, $p=0.0044$), demonstrating that neuronal activity was associated with a translocation of Lfc from dendrites to spines. B: This distribution of Lfc in spines, dendrites and axon terminals is graphed for *in vitro* slices in which activity was stimulated (n=529 profiles) or blocked (n=520), or for our perfusion fixed material (n=925) is shown. The distribution of Lfc between these three compartments differed significantly ($\chi^2=138.5$, $p<0.0001$). Post hoc testing demonstrated significant differences between all three conditions for spines and dendrites but no significant difference in the percent of Lfc found in terminals.

NIH-PA Author Manuscript
NIH-PA Author Manuscript
NIH-PA Author Manuscript

Table 1

Basic membrane properties of putative layer 2/3 projection neurons recorded from the medial prefrontal cortex of the rhesus macaque in an *in vitro* brain slice preparation. Vm = resting membrane potential; Rm = resting membrane input resistance; and Tau = the time constant (τ) of membrane charging. N = 4.

			Action Potential			
Vm (mV)	**Rm (MΩ)**	**Tau (ms)**	**Threshold (mV)**	**Amplitude (mV)**	**Rise Time (ms)**	**Half Width (ms)**
-62.8 ±0.8	52.4 ± 5.2	15.9 ± 0.4	46.9 ± 0.3	91.7 ± 0.4	0.2 ± 0.01	1.1 ± 0.02

J Comp Neurol. Author manuscript; available in PMC 2013 October 03.